

# Lattice Structure for Regular Paraunitary Linear-Phase Filterbanks and $M$ -Band Orthogonal Symmetric Wavelets

Soontorn Oraintara, *Member, IEEE*, Trac D. Tran, *Member, IEEE*, Peter Niels Heller, *Member, IEEE*, and Truong Q. Nguyen, *Senior Member, IEEE*

**Abstract**—Paraunitary linear-phase (PULP)  $M$ -channel uniform filterbanks, which are also known as the generalized lapped orthogonal transforms (GenLOTs), can be designed and implemented using lattice structures. This paper discusses how to impose regularity constraints onto the lattice structure of PULP filterbanks. These conditions are expressed in term of the rotation angles of the lattice components by which the resulting filterbanks are guaranteed to have one or two degrees of regularity. Iterating these new regular filterbanks on the lowpass subband generates a large family of symmetric  $M$ -band orthonormal wavelets. Design procedures with many design examples are presented. Smooth interpolation using regular PULP filterbanks is illustrated through image coding experiments where the novel  $M$ -band wavelets consistently yield smoother reconstructed images and better perceptual quality.

## I. INTRODUCTION

A PERFECT reconstruction (PR) filterbank (FB) provides an invertible linear time-frequency representation. Wavelets are an even more recent approach in which the filterbank is iterated to represent information at multiple scales as well as at distinct time and frequency bins. These new tools for signal processing and communications have a rich mathematical structure, introducing an entirely new collection of filter design constraints and approaches. Fig. 1(a) and (b) shows the structures of an  $M$ -channel filterbank in the regular form and its polyphase representation, respectively. For PR systems, the product of the analysis and synthesis polyphase matrices  $\mathbf{R}(\mathbf{z})\mathbf{E}(\mathbf{z})$  is equal to  $z^{-K}\mathbf{I}$ , or more generally, its pseudo-circulant version [1]. A real-coefficient filterbank is said to be *paraunitary* (PU) if  $\mathbf{R}(\mathbf{z}) = \mathbf{E}^T(\mathbf{z}^{-1})$  since  $\mathbf{E}(\mathbf{z})$  becomes a unitary matrix on the unit circle. The synthesis filters  $F_i(z)$  now become the time-reverse versions of the analysis filters  $H_i(z)$ .

Recently, PU linear-phase (PULP) filterbanks, together with the zero-tree coding framework, have been shown to yield significant improvements in still image compression

compared with other existing transforms, including the discrete cosine transform (DCT) and wavelet transform [2]–[4]. The linear-phase (LP) property of the FB allows effective representations of finite-length signals via symmetric extensions employed at signal boundaries [5]. These PULP filterbanks are also known as the lapped orthogonal transform (LOT) and its generalized version GenLOT. These terms will be used interchangeably in the paper.

PULP filterbanks are often designed and implemented using the lattice structure since the PR property can be structurally imposed. Moreover, the structure is shown to be robust, efficient, and complete. A complete and minimal factorization of PULP filterbanks is first presented in [6]. In [7], an equivalent but modular factorization is presented where the DCT and the LOT are shown to be special cases. The number of channels  $M$  is assumed to be even, and all filters have equal length of multiples of  $M$ . Theory and lattice structure for filterbanks with an odd number of channels and unequal-length filters can be found in [8], [9], and [3], respectively.

Smoothness of the scaling function, which is obtained from infinite iteration of the lowpass channel of the filterbank, is important in signal approximation and interpolation. The smoothness of the scaling function is closely related to the concept of *regularity*, which is defined as the number of zeros at mirror (aliasing) frequencies  $2k\pi/M$ ,  $k = 1, 2, \dots, M-1$  of the lowpass filter [10]. Systems with higher degree of regularity have smoother scaling functions. Note that the degree of regularity of the filterbanks is defined from the scaling function viewpoint. From the wavelet-function perspective, this property is known as the *vanishing moment* because the corresponding wavelets are orthogonal to any piecewise polynomial of degree  $K-1$ , where  $K$  is the number of vanishing moments (equivalently, the degrees of regularity). In other words, all filters except the lowpass  $H_0(z)$  must have a zero of order  $K$  at dc frequency ( $\omega = 0$ ) [10].

From the iterative construction of wavelets, it has been proven for the dyadic case ( $M = 2$ ) that one vanishing moment is a necessary condition for the convergence of the scaling function and the mother wavelet [11]. This is equivalent to the zero frequency response at  $\pi$  of the lowpass filter. In the case of  $M$ -band wavelets, the frequency response of the lowpass filter is  $H_0(W^k) = 0$  for all  $1 \leq k \leq M-1$  and  $W = e^{j(2\pi/M)}$ . Consequently, the scaling function  $\phi(t)$  can exactly represent a (piecewise) constant signal. Moreover, if the lowpass filter is  $K$ -regular, the scaling function  $\phi(t)$  can exactly represent any

Manuscript received September 18, 2000; revised July 16, 2001. The associate editor coordinating the review of this paper and approving it for publication was Dr. Helmut Boelskei.

S. Oraintara is with the the Electrical Engineering Department, University of Texas at Arlington, Arlington, TX 76011 USA (e-mail: oraintar@uta.edu).

T. D. Tran is with the Electrical Engineering Department, The John Hopkins University, Baltimore MD 21218 USA (e-mail: trac@thanglong.ece.jhu.edu).

P. N. Heller is with Aware, Inc., Bedford MA 01730 USA (e-mail: heller@aware.com).

T. Q. Nguyen is with the Electrical and Computer Engineering Department, University of California–San Diego, La Jolla, CA 92093 USA (e-mail: nguyent@ece.ucsd.edu).

Publisher Item Identifier S 1053-587X(01)09228-5.

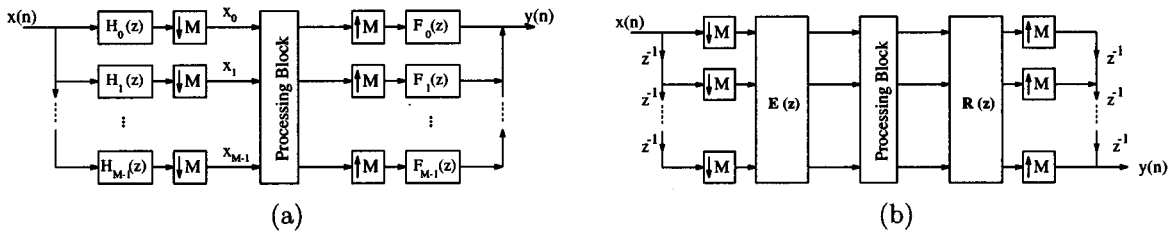


Fig. 1. Block diagram of  $M$ -channel filterbanks. (a) Filter structure and (b) its equivalent polyphase structure.

polynomial up to degree  $K - 1$ . Hence, this property is very important in smooth signal approximation application such as image coding and denoising.

Despite the elegance of regularity, lattice structures for regular PULP filterbanks have not been reported in the literature. In the case when  $M = 2$ , it is well known that PU and LP are exclusive properties (except for the simple Haar wavelet). All two-band solutions have been found, and each of them has its own lattice structure [12], [13]. For the two-channel PU case, the filterbank has one regularity if all rotation angles in the structure sum up to  $\pi/4$  [2]. This paper aims to generalize the above two-band result: investigating the lattice structure of  $M$ -channel regular PULP filter banks. Preliminary results can also be found in [14]. Throughout this paper, the number of channels  $M$  is assumed to be even, and the length of all filters is restricted to an integer multiple of  $M$ . It has been proven that when  $M$  is even, an  $M$ -channel filter bank with linear-phase consists of an equal number of symmetric and anti-symmetric filters [6]. Since the anti-symmetric filters already have one zero at  $\omega = 0$ , one expects that for the first vanishing moment, the regularity condition needs to be imposed into the  $M/2$  symmetric filters only.

Two conventional approaches in designing  $M$ -channel regular filterbanks have been suggested. The first method is to impose the number of zeros at mirror frequencies into the lowpass filter [10], [15]. Having constructed the first filter, the remaining  $M - 1$  filters have to be designed such that the overall resulting filterbank is PR. For the two-channel case, the highpass channel can be uniquely determined from the lowpass filter, whereas for  $M > 2$ , there are more degrees of freedom in choosing the bandpass and the highpass filters. This later step can be accomplished using a Gram-Schmidt process [10], [16]. However, this approach does not guarantee the linear-phase property of the filters. Moreover, the resulting filterbank is not globally optimum since one of the filters has been preselected. Another method is to use time-domain constraints [17]. A PR filterbank is first constructed, possibly using the lattice structure. Then, vanishing-moment conditions are enforced by time-domain side-constraints. The disadvantage of this *ad hoc* approach is that the optimization process becomes significantly more complicated, leading to slow convergence (if at all), and the optimization process can easily get trapped in local minima. Moreover, regularity can only be approximately imposed.

#### A. Organization

In this paper, we present a novel approach of imposing up to two vanishing moments directly onto the lattice structure of  $M$ -channel PULP filterbanks. We begin with a review of the

lattice structure for PULP filterbanks in Section II. Next, various necessary conditions for  $K$ -regular  $M$ -channel filterbanks are derived in Section III. Section IV discusses the first and second vanishing moments in terms of the lattice coefficients. The equivalent relations on the rotation angles of the lattice structure are derived so that the resulting filterbank is guaranteed to have  $K$  degrees of regularity along with the PULP property. Design examples are presented throughout. Section V presents image coding experiments where the new regular FBs and  $M$ -band wavelets consistently yield more visually pleasant reconstructed images. Finally, concluding remarks are found in Section VI.

#### B. Notations

Boldfaced lower-case characters are used to denote vectors, whereas boldfaced upper-case characters are used to denote matrices.  $\mathbf{A}^T$ ,  $\mathbf{A}^{-1}$ ,  $|\mathbf{A}|$ ,  $\mathbf{A}_i$ ,  $\mathbf{A}_j$ , and  $a_{ij}$  denote, respectively, the transpose, the inverse, the determinant, the  $i$ th row, the  $j$ th column, and the  $i$ th  $j$ th element of the matrix  $\mathbf{A}$ . The symbols  $h_i[n]$ ,  $H_i(z)$ , and  $H_i(e^{j\omega})$  stand for the  $i$ th filter's impulse response, its associated  $z$ -transform, and its Fourier transform.

Several special matrices with reserved symbols are the polyphase matrix of the analysis bank  $\mathbf{E}(z)$ , the polyphase matrix of the synthesis bank  $\mathbf{R}(z)$ , the identity matrix  $\mathbf{I}$ , the reversal matrix  $\mathbf{J}$  ( $\mathbf{I}$  flipped left-right or up-down), the null matrix  $\mathbf{0}$ , a permutation matrix  $\mathbf{P}$ , and the diagonal matrix with entries being either  $+1$  or  $-1$   $\mathbf{D}$ . Likewise, the special vectors are the column vector with all entries being unity  $\mathbf{1}$  and the column vector with all entries being zero, except the first entry being one  $\mathbf{a}$ . When the size of a matrix or vector is not clear from context, subscripts will be included.  $M$  and  $K$  are usually reserved for the number of channels and the degrees of regularity. An  $M$ -channel  $MN$ -tap FB is sometimes denoted as an  $M \times MN$  lapped transform, where  $N$  is the overlapping factor. For abbreviations, we often use LP, PR, PU, and FB to denote *linear phase*, *perfect reconstruction*, *paraunitary*, and *filterbank*.

## II. LATTICE STRUCTURE FOR PULP FILTER BANKS: A REVIEW

Lattice structure is an efficient implementation of PULP filterbanks where both the PU and LP properties are simultaneously imposed into the filters' impulse responses. It is assumed that the number of channels  $M \geq 4$  is even, and all the filters have equal length  $\ell = NM$ , where  $N$  is an integer. It has been proven that when the number of channels is even, there are  $M/2$  symmetric and  $M/2$  anti-symmetric filters [4], [6]. The

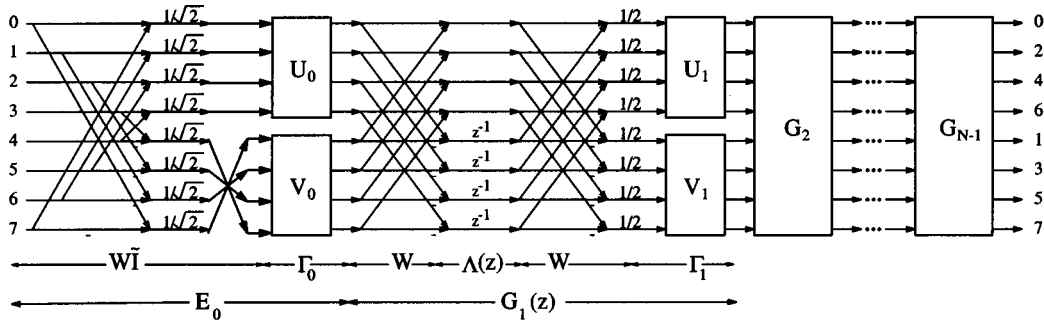


Fig. 2. Lattice structure for PULP filterbanks (GenLOT).

polyphase matrix  $\mathbf{E}(z)$  is a degree  $N - 1$  polynomial matrix in  $z$ . Under the assumptions on  $M$ ,  $N$ , and the filter symmetry, define the lattice elements as

$$\mathbf{\Gamma}_i = \begin{bmatrix} \mathbf{U}_i & \mathbf{0}_L \\ \mathbf{0}_L & \mathbf{V}_i \end{bmatrix}, \quad \mathbf{W} = \frac{1}{\sqrt{2}} \begin{bmatrix} \mathbf{I}_L & \mathbf{I}_L \\ \mathbf{I}_L & -\mathbf{I}_L \end{bmatrix},$$

$$\mathbf{\Lambda}(z) = \begin{bmatrix} \mathbf{I}_L & \mathbf{0}_L \\ \mathbf{0}_L & z^{-1}\mathbf{I}_L \end{bmatrix}, \quad \text{and} \quad \tilde{\mathbf{I}} = \begin{bmatrix} \mathbf{I}_L & \mathbf{0}_L \\ \mathbf{0}_L & \mathbf{J}_L \end{bmatrix}$$

where  $L = M/2$ , and  $\mathbf{J}$  is the reversal matrix.  $\mathbf{U}_i$  and  $\mathbf{V}_i$  are orthonormal matrices of size  $L \times L$ , and each can be parameterized using  $\binom{L}{2}$  rotation angles [1]. The polyphase matrix  $\mathbf{E}(z)$  of a PULP filterbank with degree  $N - 1$  can always be factored as a product of PU matrices with degree one [7], i.e.,

$$\mathbf{E}(z) = \mathbf{G}_{N-1}(z)\mathbf{G}_{N-2}(z)\cdots\mathbf{G}_1(z)\mathbf{E}_0 \quad (1)$$

where  $\mathbf{G}_i(z) = \mathbf{\Gamma}_i\mathbf{W}\mathbf{\Lambda}(z)\mathbf{W}$ , and  $\mathbf{E}_0 = \mathbf{\Gamma}_0\mathbf{W}\tilde{\mathbf{I}}$ . Fig. 2 shows the complete lattice structure of PULP filterbanks. Although this structure is minimal in terms of the number of delays, it does not minimize the number of free parameters. In [18], the authors show that the matrices  $\mathbf{U}_i$  for  $i > 0$  can be set to  $\mathbf{I}$  without any completeness violation. This more efficient structure with

$$\mathbf{U}_i \equiv \mathbf{I} \quad \text{for } i > 0$$

will be used in the analysis of the forthcoming sections.

Having characterized the PULP filterbanks this way, one can view the discrete cosine transform (DCT) and lapped orthogonal transform (LOT) as special cases with  $N = 1$  and  $N = 2$ , respectively. This is the reason why the structure is called Generalized LOT (GenLOT). Fig. 3 shows an example of parameterization of orthogonal matrices. It should be noted that while the above parameterization of orthogonal matrices is complete, it is not unique, i.e., one can parameterize the same matrix with different order of rotation angles.

### III. LATTICE STRUCTURE FOR REGULAR PULP FILTERBANKS

*Definition III.1:* A filterbank has  $K$  degrees of regularity if its lowpass filter  $H_0(z)$  has  $K$  multiple zeros at each mirror frequency  $2\pi k/M$  for  $1 \leq k \leq M - 1$ .

The above condition is sometime called vanishing moment of the filterbank since it is equivalent to the number of zeros at dc of the bandpass filters. In particular, it can be proven that in a

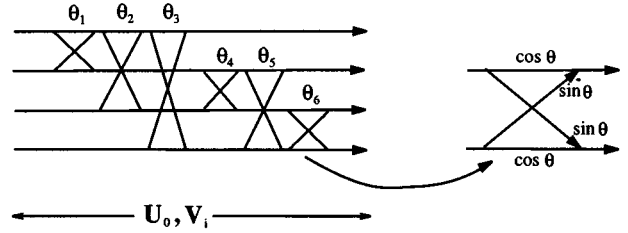


Fig. 3. Orthogonal matrix parameterization.

PU filterbank, the lowpass filter  $H_0(z)$  has  $K$  multiple zeros at each mirror frequency if and only if the bandpass filter  $H_i(z)$  has  $K$  multiple zeros at  $z = 1$  for  $1 \leq i \leq M - 1$  [10].

*Theorem III.1:* A filterbank has  $K$  degrees of regularity if and only if its polyphase matrix  $\mathbf{E}(z)$  satisfies the following condition:

$$\frac{d^n}{dz^n} \left\{ \mathbf{E}(z^M) \begin{bmatrix} 1 \\ z^{-1} \\ \vdots \\ z^{1-M} \end{bmatrix} \right\} \Big|_{z=1} = \begin{bmatrix} c_n \\ 0 \\ \vdots \\ 0 \end{bmatrix} \quad (2)$$

where  $c_n$  are some nonzero constants for  $n = 0, \dots, K - 1$  [19].

*Theorem III.2:* A filterbank parameterized by the lattice structure presented in Fig. 2 has one regularity if and only if

$$\mathbf{A}_0: \mathbf{U}_0\mathbf{1}_L = \sqrt{L}\mathbf{a}_L. \quad (3)$$

*Proof:* From Theorem III.1, in order to obtain the first regularity of the bandpass/highpass filters, the polyphase matrix must satisfy

$$\mathbf{E}(1)\mathbf{1}_M = \left\{ \mathbf{E}(z^M) \begin{bmatrix} 1 \\ z^{-1} \\ \vdots \\ z^{-M+1} \end{bmatrix} \right\} \Big|_{z=1} = \begin{bmatrix} c_0 \\ 0 \\ \vdots \\ 0 \end{bmatrix}.$$

Since

$$\mathbf{E}(1) = \mathbf{\Gamma}_{N-1}\mathbf{\Gamma}_{N-2}\cdots\mathbf{\Gamma}_0\mathbf{W}\tilde{\mathbf{I}} = \begin{bmatrix} \mathbf{U}_0 & & \\ & \prod_{i=N-1}^0 \mathbf{V}_i & \\ & & \end{bmatrix} \mathbf{W}\tilde{\mathbf{I}}$$

hence

$$\begin{aligned} \mathbf{E}(1)\mathbf{1}_M &= \begin{bmatrix} \mathbf{U}_0 \\ \prod_{i=N-1}^0 \mathbf{V}_i \end{bmatrix} \mathbf{W}\mathbf{1}_M \\ &= \sqrt{2} \begin{bmatrix} \mathbf{U}_0 \\ \prod_{i=N-1}^0 \mathbf{V}_i \end{bmatrix} \begin{bmatrix} \mathbf{1}_L \\ \mathbf{0}_L \end{bmatrix} \\ &= \sqrt{2} \begin{bmatrix} \mathbf{U}_0 \mathbf{1}_L \\ \mathbf{0}_L \end{bmatrix} = \mathbf{c}_0 \mathbf{a}_M \end{aligned}$$

where we are reminded that  $\mathbf{a} = [\mathbf{1} \ \mathbf{0} \ \mathbf{0} \ \dots \ \mathbf{0}]^T$ . Using the fact that  $\mathbf{U}_0$  is orthogonal, it is clear that  $c_0 = \pm\sqrt{M}$ . Without loss of generality, we assume that the dc value of the lowpass filter is positive, which implies that  $c_0 = \sqrt{M}$ . ■

Note that the above condition  $A_0$  does not depend on the matrices  $\mathbf{V}_i$  because of the fact that the  $L$  filters  $H_L(z)$ ,  $H_{L+1}(z), \dots, H_{M-1}(z)$  are antisymmetric filters, and therefore, their frequency responses at  $\omega = 0$  are zero. From (3), it is clear that the matrix  $\mathbf{U}_0$  rotates the vector  $\mathbf{1}_L$  while preserving its norm to the vector  $\sqrt{L} \mathbf{a}_L$ . This step can be done by properly choosing the orders and values of  $L-1$  rotation angles from the parameterization of the matrix  $\mathbf{U}_0$ , as discussed in the next section.

*Theorem III.3:* If the filterbank in Fig. 2 (with  $\mathbf{U}_i = \mathbf{I}$  for  $i > 0$ ) satisfies the condition  $A_0$ , it has two degrees of regularity if and only if it satisfies the following condition:

$$A_1: \sqrt{L} \mathbf{a}_L + \sqrt{L} \sum_{j=2}^{N-1} \prod_{i=N-2}^{N-j} \mathbf{V}_i \mathbf{a}_L + \prod_{i=N-2}^0 \mathbf{V}_i \mathbf{b} = \mathbf{0}_L \quad (4)$$

where  $\mathbf{b} = (1/M)[\mathbf{1} \ \mathbf{3} \ \mathbf{5} \ \dots \ \mathbf{M} - \mathbf{1}]^T$ .

*Proof:* Since the proof is straightforward but cumbersome, we defer it to the Appendix. We may proceed without any discontinuity. ■

*Theorem III.4:* The minimal length for a two-regular PULP filterbank is  $3M$ .

*Proof:* Keep in mind that in order for the filter bank to have two degrees of regularity, both conditions  $A_0$  and  $A_1$  must be satisfied. The first condition can be satisfied by choosing  $\mathbf{U}_0$  properly. The second condition composes of  $N$  vectors forming a closed loop (zero sum). Taking into account that  $\mathbf{V}_i$  are orthogonal matrices, the first  $N-1$  vectors in (4) have equal length  $\sqrt{L} = \sqrt{M/2}$ , and the last vector has length  $\|\mathbf{b}\| = \sqrt{1^2 + 3^2 + \dots + (2L-1)^2}/M = \sqrt{(M^2-1)/6M} \neq \sqrt{M/2}$ . Therefore, in order for the condition  $A_1$  to hold, there must be at least three vectors, i.e.,  $N \geq 3$ . This proves that the minimal length for PULP filterbanks with two vanishing moments is  $3M$ . ■

The  $N$  vectors in (4) form a closed loop, and hence, they must obey the triangle inequality. In particular, since the matrices  $\mathbf{V}_i$  are orthonormal, the lengths of the  $N$  vectors are fixed, and these matrices can only control the directions of these vectors. For example, given a choice of  $\mathbf{V}_i$  for  $i = 0, \dots, N-3$ , it is not clear if there exists  $\mathbf{V}_{N-2}$  that satisfies (4). In the next section, the condition  $A_1$  is divided into three cases based on the length of the filters to ensure that the triangle inequality holds at all

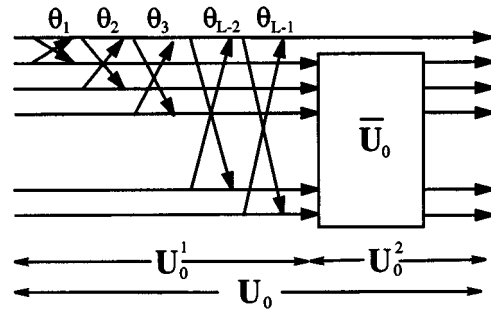


Fig. 4. Parameterization of the orthogonal matrices  $\mathbf{U}_0$ .

time. The first case is the minimal length case ( $N = 3$ ), where there are only three vectors in the condition  $A_1$  forming a fixed triangle (all interior angles are fixed and known). The second case is when the length of the filters is  $4M$  ( $N = 4$ ), where there are four vectors presented in the condition  $A_1$ . In this case, the interior angles of the quadrilateral are not fixed and depend on the choices of  $\mathbf{V}_i$ . The last case is the generalization of the first two cases by which the length of the filters can be extended to arbitrary multiple of  $M$ .

#### IV. REGULARITY IMPOSITION INTO THE LATTICE STRUCTURE

##### A. Imposing the First Regularity

The condition  $A_0$  in (3) implies that every row of  $\mathbf{U}_0$  except for the top one is orthogonal to  $\mathbf{1}$ . Since  $\mathbf{U}_0$  is orthonormal, one concludes that its top row must be constant and is equal to  $1/\sqrt{L}$ . Note that the popular DCT matrix used in JPEG and MPEG standards satisfies this condition. Let us parameterize the matrix  $\mathbf{U}_0$  as in Fig. 4. Note that since the order of the rotation angles is not unique, the configuration in Fig. 4 is chosen for convenience of the rest of the development. We divide the  $\binom{L}{2}$  rotation angles of  $\mathbf{U}_0$  into two parts. The first  $L-1$  rotations angles  $\theta_j$  operate between the first row and the others, and the other  $\binom{L}{2} - (L-1) = \binom{L-1}{2}$  rotation angles reside in the  $(L-1) \times (L-1)$  matrix  $\bar{\mathbf{U}}_0$  operating on the bottom  $L-1$  rows, as indicated in Fig. 4. It is easy to see that (3) can be enforced by using  $L-1$  out of  $\binom{L}{2}$  degrees of freedom of  $\mathbf{U}_0$  as follows.

*Theorem IV.1:* Let  $\mathbf{U}_0$  be parameterized as in Fig. 4.  $\mathbf{U}_0 \mathbf{1}_L = \sqrt{L} \mathbf{a}_L$  if and only if the following conditions hold:

- 1)  $\theta_1 = -\tan^{-1} 1$ .
- 2)  $\theta_i = \pm \tan^{-1}(1/\sqrt{i})$  for  $i = 2, \dots, L-2$ .
- 3)  $\theta_{L-1} = -\sin^{-1}(1/\sqrt{L})$ .

*Proof:* Since  $\mathbf{U}_0^T \mathbf{a}_L = \mathbf{1}_L$ , it is sufficient to show that  $\mathbf{U}_0 \mathbf{1}_L = \sqrt{L} \mathbf{a}_L$ . Since the second element of  $\mathbf{a}_L$  is zero, from Fig. 4, it is obvious that

$$\begin{aligned} \sin \theta_1 + \cos \theta_1 = 0 &\Rightarrow \theta_1 = -\tan^{-1} 1 \\ &\Rightarrow \cos \theta_1 - \sin \theta_1 = \pm\sqrt{2}. \end{aligned}$$

Similarly, considering the third element of  $\mathbf{a}_L$ , which is zero, we have

$$\begin{aligned} \pm\sqrt{2} \sin \theta_2 + \cos \theta_2 = 0 &\Rightarrow \theta_2 = \mp \tan^{-1} \frac{1}{\sqrt{2}} \\ &\Rightarrow \pm\sqrt{2} \cos \theta_2 - \sin \theta_2 = \pm\sqrt{3}. \end{aligned}$$

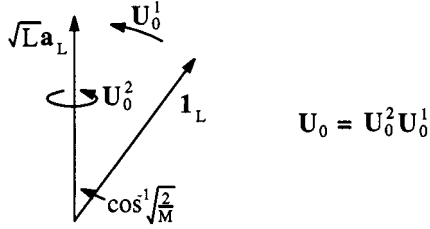


Fig. 5. Role of the matrix  $\mathbf{U}_0$  for the first regularity.

Keep repeating the same procedure for all  $\theta_i$  until  $i = L - 2$ . When  $i = L - 1$ , we have

$$\begin{aligned} & \pm\sqrt{L-1} \cos \theta_{L-1} - \sin \theta_{L-1} \\ &= \pm\sqrt{L-1} \left( \pm \frac{\sqrt{L-1}}{\sqrt{L}} \right) - \sin \theta_{L-1} \\ &= \sqrt{L} \Rightarrow \theta_{L-1} = -\sin^{-1} \frac{1}{\sqrt{L}}. \quad \blacksquare \end{aligned}$$

### 1) Geometry Interpretation:

*Definition IV.1:* The angle between two vectors  $\mathbf{p}$  and  $\mathbf{q}$  is defined by

$$\angle(\mathbf{p}, \mathbf{q}) = \cos^{-1} \left( \frac{\mathbf{p}^T \mathbf{q}}{\|\mathbf{p}\| \|\mathbf{q}\|} \right).$$

*Fact 1:* The angle between any two vectors does not depend on their lengths, i.e.,  $\angle(c_1 \mathbf{p}, c_2 \mathbf{q}) = \angle(\mathbf{p}, \mathbf{q})$ , where  $c_1$  and  $c_2$  are both positive (or both negative) scalar constants.

*Fact 2:* The angle is preserved under a rigid rotation, i.e., if  $\mathbf{D}$  is an orthogonal matrix, then  $\angle(\mathbf{D}\mathbf{p}, \mathbf{D}\mathbf{q}) = \angle(\mathbf{p}, \mathbf{q})$ , where we have used the fact that  $\mathbf{D}^T \mathbf{D} = \mathbf{I}$ .

From (3), it is clear that the matrix  $\mathbf{U}_0$  rotates, while preserving the norm, the vector  $\mathbf{1}_L$  into the direction of vector  $\mathbf{a}_L$ . Note that the angle between  $\mathbf{1}_L$  and  $\mathbf{a}_L$  is

$$\begin{aligned} \gamma = \angle(\mathbf{1}_L, \mathbf{a}_L) &= \cos^{-1} \frac{\mathbf{1}_L^T \mathbf{a}_L}{\|\mathbf{1}_L\| \|\mathbf{a}_L\|} \\ &= \cos^{-1} \frac{1}{\sqrt{L}} = \cos^{-1} \sqrt{\frac{2}{M}}. \end{aligned}$$

Fig. 5 illustrates the roles of  $\mathbf{U}_0^1$  and  $\mathbf{U}_0^2$  in  $\mathbf{U}_0$ . The first  $L-1$  rotation angles in  $\mathbf{U}_0^1$  rotate the vector  $\mathbf{1}_L$  to the direction of  $\mathbf{a}_L$ . Then,  $\mathbf{U}_0^2$  rotates the resulting vector in the direction perpendicular to  $\mathbf{a}_L$ , and thus, the resulting vector remains the same.

2) *Design Example:* In this example, a one-regular eight-channel 24-tap PULP filterbank is designed using the lattice structure. The filters are optimized in order to maximize the stopband attenuation, which can be given by

$$C_{\text{stopband attn.}} = - \sum_{i=0}^{M-1} \int_{\Omega_i} [W_i(e^{j\omega}) |H_i(e^{j\omega})|^2 d\omega]$$

where  $W_i(e^{j\omega})$  are some weighting functions, and  $\Omega_i$  are stopband regions of the filters. Fig. 6(a) shows the frequency responses of the resulting filters. The zeros of the lowpass filter are plotted in Fig. 6(b), showing that the filterbank has one degree of regularity, which confirms the theory. Fig. 6(c) shows the corresponding scaling function and wavelets.

### B. Imposing the Second Regularity: Minimal Length Case

Supposing that the first regularity has been imposed into  $\mathbf{U}_0$  of the PULP filterbank, we now discuss how to impose the second regularity using the condition  $A_1$ . Let us take the simplest case when the filter length is minimal. From Theorem III.4, the minimal length for PULP filterbanks with two vanishing moments is  $3M$ , where  $M$  is the number of channels. Substituting  $N = 3$  into (4), we have

$$\sqrt{L} \mathbf{a}_L + \sqrt{L} \mathbf{V}_1 \mathbf{a}_L + \mathbf{V}_1 \mathbf{V}_0 \mathbf{b} = \mathbf{0}_L. \quad (5)$$

The question is now as follows: How can one choose the rotation angles in  $\mathbf{V}_i$  so that (5) is satisfied? For convenience, let  $\mathbf{x}_1 = \sqrt{L} \mathbf{a}_L$ ,  $\mathbf{x}_2 = \sqrt{L} \mathbf{V}_1 \mathbf{a}_L$ , and  $\mathbf{x}_3 = \mathbf{V}_1 \mathbf{V}_0 \mathbf{b}$ . These three vectors form a bilateral triangle with  $\|\mathbf{x}_1\| = \|\mathbf{x}_2\| = \sqrt{L}$ , as depicted in Fig. 7. Having known the three sides of the triangle, one can determine the angles between each pair of the three vectors. Letting  $\lambda$ ,  $\lambda_1$ , and  $\lambda_2$  be defined as in Fig. 7, it is easy to see that

$$\begin{aligned} \lambda_1 &= 2 \sin^{-1} \left( \frac{1}{2M} \sqrt{\frac{M^2-1}{3}} \right) \\ \lambda_2 &= \cos^{-1} \left( \frac{1}{2M} \sqrt{\frac{M^2-1}{3}} \right), \quad \text{and} \quad \lambda = \lambda_1 + \lambda_2. \end{aligned}$$

From the above definitions of  $\mathbf{x}_i$  and Fig. 7, we have

$$\begin{aligned} \lambda = \lambda_1 + \lambda_2 &= \angle(\mathbf{x}_2, \mathbf{x}_3) = \angle(\mathbf{V}_1 \mathbf{a}_L, \mathbf{V}_1 \mathbf{V}_0 \mathbf{b}) \\ &= \angle(\mathbf{a}_L, \mathbf{V}_0 \mathbf{b}) \end{aligned} \quad (6)$$

where the last equation is obtained by left-multiplying both vectors by  $\mathbf{V}_1^T$ . From (6), it is clear that the angle between the vectors  $\mathbf{x}_2$  and  $\mathbf{x}_3$  is dependent on the matrix  $\mathbf{V}_0$  only. *This is the key of how to parameterize the matrix  $\mathbf{V}_0$ .* Supposing that  $\mathbf{V}_0$  satisfies (6), we have  $\angle(\mathbf{x}_2, \mathbf{x}_3) = \lambda$ , which implies that  $\|\mathbf{x}_2 + \mathbf{x}_3\| = \sqrt{L} = \|\mathbf{x}_1\|$ , permitting the matrix  $\mathbf{V}_1$  to be able to close the triangle by properly rotating the vector  $\mathbf{a}_L + \mathbf{V}_0 \mathbf{b}$ .

*Definition IV.2:* Let  $\mathbf{R}[\mathbf{p}]$  be an  $L \times L$  orthogonal matrix defined on the  $L \times 1$  vector  $\mathbf{p}$  as follows:

$$\mathbf{R}[\mathbf{p}] = \mathbf{I} - 2 \frac{\mathbf{v}_p \mathbf{v}_p^T}{\|\mathbf{v}_p\|^2} \quad (7)$$

where  $\mathbf{v}_p = (\mathbf{p}/\|\mathbf{p}\|) - \mathbf{a}_L$ . This matrix is called the *Householder matrix* [20], which maps the vector  $\mathbf{p}$  into the direction of  $\mathbf{a}_L$  while preserving its norm, i.e.,

$$\mathbf{R}[\mathbf{p}]\mathbf{p} = \|\mathbf{p}\| \mathbf{a}_L.$$

1) *Parameterization of  $\mathbf{V}_0$ :* From (6), we have

$$\lambda = \angle(\mathbf{x}_2, \mathbf{x}_3) = \angle(\mathbf{a}_L, \mathbf{V}_0 \mathbf{b}) = \angle(\mathbf{a}_L, \mathbf{V}_0 \mathbf{R}[\mathbf{b}]^T \mathbf{a}_L). \quad (8)$$

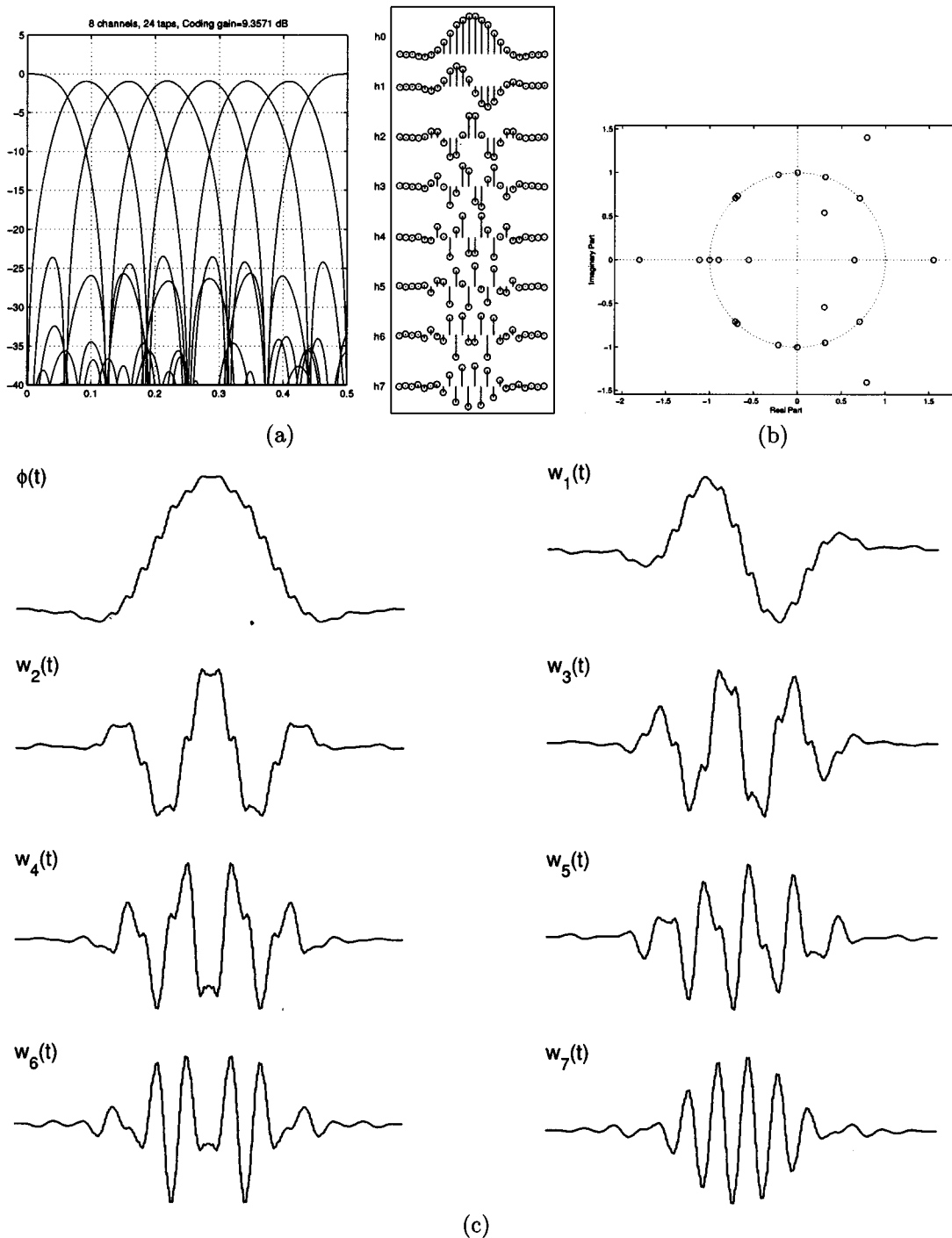


Fig. 6. Design example eight-channel PULP filterbank with one vanishing moment. (a) Frequency and impulse responses. (b) Zero locations of the lowpass filter. (c) Scaling function and wavelets.

Let us parameterize  $V_0$  as in Fig. 8, i.e.,

$$V_0 = V_0^2 V_0^1 V_0^0.$$

By choosing  $V_0^0 = R[b]$ , (8) then implies

$$\lambda = \angle(a_L, V_0^2 V_0^1 a_L) = \angle(V_0^{2T} a_L, V_0^1 a_L) = \angle(a_L, V_0^1 a_L) \quad (9)$$

where in the last equation, we have used the fact that

$$V_0^{2T} a_L = \begin{pmatrix} 1 & 0 \\ 0 & V_0^T \end{pmatrix} a_L = a_L.$$

It should be noted that the above parameterization does not increase the degree of freedom from  $\binom{L}{2}$  since  $V_0^0$  is fixed.

*Theorem IV.2:*  $V_0^1(1, 1) = \cos \lambda$ .

*Proof:* From (9), it is clear that

$$\cos \lambda = \frac{a_L^T V_0^1 a_L}{\|a_L\| \|V_0^1 a_L\|} = \frac{V_0^1(1, 1)}{\|a_L\|^2} = V_0^1(1, 1). \quad \blacksquare$$

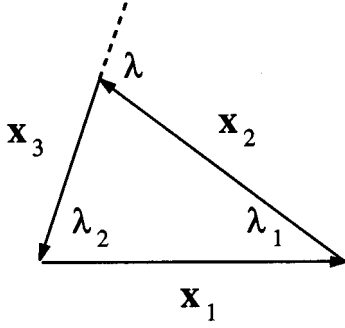


Fig. 7. Geometrical interpretation of (5), where the three vectors  $\mathbf{x}_1$ ,  $\mathbf{x}_2$ , and  $\mathbf{x}_3$  form a triangle.

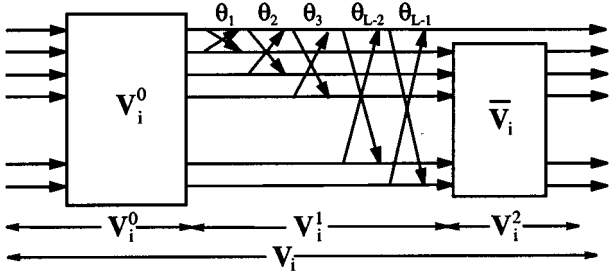


Fig. 8. Parameterization of the orthogonal matrices  $\mathbf{V}_i$ .

Let the  $\binom{L}{2}$  rotation angles of the matrix  $\mathbf{V}_0^1$  and  $\mathbf{V}_0^2$  be ordered as in Fig. 8, where  $\bar{\mathbf{V}}_0$  is an orthogonal matrix of size  $(L-1) \times (L-1)$  consisting of  $\binom{L}{2} - (L-1) = \binom{L-1}{2}$  rotation angles. From Fig. 8, it is easy to show that  $\mathbf{V}_0^1(\mathbf{1}, \mathbf{1}) = \cos \lambda$  if and only if

$$\cos \theta_1 \cos \theta_2 \cdots \cos \theta_{L-1} = \cos \lambda. \quad (10)$$

Since (10) is independent from the matrix  $\bar{\mathbf{V}}_0$ , the  $\binom{L-1}{2}$  rotation angles of  $\bar{\mathbf{V}}_0$  can be arbitrarily chosen, and the resulting matrix  $\mathbf{V}_0^1$  still satisfies (9). In order to satisfy (10), clearly, the degree of freedom of  $\mathbf{V}_0$  is reduced by one. Having parameterized as above, the resulting angle between  $\mathbf{x}_2$  and  $\mathbf{x}_3$  is equal to  $\lambda$ , and hence,  $\|\mathbf{x}_2 + \mathbf{x}_3\| = \sqrt{L} = \|\mathbf{x}_1\|$ .

2) *Parameterization of  $\mathbf{V}_1$* : Having specified  $\mathbf{V}_0$ , what remains in (5) is how to choose  $\mathbf{V}_1$  so that  $\mathbf{x}_1 = -\mathbf{x}_2 - \mathbf{x}_3$ . This step takes out  $L-1$  degrees of freedom from  $\mathbf{V}_1$ , as in the case of imposing the first vanishing moment into  $\mathbf{U}_0$ . From (5)

$$\begin{aligned} \sqrt{L} \mathbf{a}_L &= \mathbf{V}_1(-\sqrt{L} \mathbf{a}_L - \mathbf{V}_0 \mathbf{b}) \\ &= \|-\sqrt{L} \mathbf{a}_L - \mathbf{V}_0 \mathbf{b}\| \mathbf{V}_1 \mathbf{R}[-\sqrt{L} \mathbf{a}_L - \mathbf{V}_0 \mathbf{b}]^T \mathbf{a}_L \\ &= \sqrt{L} \mathbf{V}_1 \mathbf{R}[-\sqrt{L} \mathbf{a}_L - \mathbf{V}_0 \mathbf{b}]^T \mathbf{a}_L \end{aligned} \quad (11)$$

where in the last equation, we have used the fact that  $\|-\sqrt{L} \mathbf{a}_L - \mathbf{V}_0 \mathbf{b}\| = \sqrt{L}$ . Let  $\mathbf{V}_1$  be parameterized as in Fig. 8, i.e.,

$$\mathbf{V}_1 = \mathbf{V}_1^2 \mathbf{V}_1^1 \mathbf{V}_1^0.$$

By choosing  $\mathbf{V}_1^0 = \mathbf{R}[-\sqrt{L} \mathbf{a}_L - \mathbf{V}_0 \mathbf{b}]$ , then (11) implies

$$\mathbf{a}_L = \mathbf{V}_1^2 \mathbf{V}_1^1 \mathbf{a}_L = \mathbf{V}_1^1 \mathbf{a}_L \quad (12)$$

where in the last equation, we have used the fact that

$$\mathbf{V}_1^2 \mathbf{a}_L = \begin{pmatrix} 1 & 0 \\ 0 & \mathbf{V}_1^T \end{pmatrix} \mathbf{a}_L = \mathbf{a}_L.$$

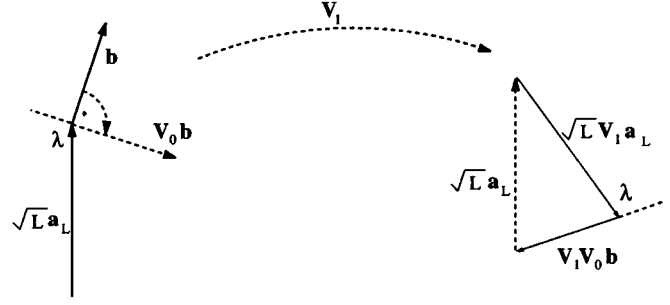


Fig. 9. Role of the matrices  $\mathbf{V}_i$  for the second vanishing moment.

Similar to the case of  $\mathbf{V}_0$ , this parameterization does not increase the degree of freedom from  $\binom{L}{2}$  since the matrix  $\mathbf{V}_0$  has already been determined, and hence, the choice of  $\mathbf{V}_1^0$  is fixed.

3) *Geometric Interpretation of the  $\mathbf{V}_i$  Matrices*: For the second vanishing moment, the condition is a little more complicated, but the geometry is still simple. In this case, there are three vectors forming a closed bilateral triangle as in Fig. 7, where the values of  $\lambda$ ,  $\lambda_1$ , and  $\lambda_2$  are uniquely determined as follows:

$$\lambda_1 = 2 \sin^{-1} \left( \frac{1}{2M} \sqrt{\frac{M^2 - 1}{3}} \right),$$

$$\lambda_2 = \cos^{-1} \left( \frac{1}{2M} \sqrt{\frac{M^2 - 1}{3}} \right), \quad \text{and} \quad \lambda = \lambda_1 + \lambda_2.$$

By rewriting (5) as

$$\sqrt{L} \mathbf{a}_L + \mathbf{V}_1 [\sqrt{L} \mathbf{a}_L + \mathbf{V}_0 \mathbf{b}] = \mathbf{0}_L$$

the following observations can be made (see Fig. 9).

- 1)  $\mathbf{V}_0$  must rotate  $\mathbf{b}$  in such a way that the angle between  $\mathbf{V}_0 \mathbf{b}$  and  $\mathbf{a}_L$  is  $\lambda$ .
- 2)  $\mathbf{V}_1$  rotates the two vectors  $\sqrt{L} \mathbf{a}_L$  and  $\mathbf{V}_0 \mathbf{b}$  together so that the resulting vector is in the direction of  $-\mathbf{a}_L$ .

4) *Design Example*: In this example, a two-regular eight-channel PULP filterbank is designed with minimal length, i.e., all the filters have length  $\ell = 3 \times 8 = 24$ . The frequency responses are presented in Fig. 10(a), and the zeros of the low-pass filters are plotted in Fig. 10(b). Fig. 10(c) shows the corresponding scaling function and wavelets. It can be seen that the lowpass filter has (at least) double zeros at each the mirror frequencies, which confirms that the bandpass and highpass filters will have (at least) two vanishing moments. In this design example, the stopband attenuation is used to optimize the filters. One observes that frequency response of this filterbank has lower stopband attenuation than that of the one in the design example 1. This is simply because of the fact that a number of free parameters have been used to impose the second vanishing moment.

*C. Imposing the Second Regularity: Filter Length Is Equal to  $4M$  ( $N = 4$ )*

Substituting  $N = 4$  into the condition  $A_1$  yields

$$\sqrt{L} [\mathbf{a}_L + \mathbf{V}_2 \mathbf{a}_L + \mathbf{V}_2 \mathbf{V}_1 \mathbf{a}_L] + \mathbf{V}_2 \mathbf{V}_1 \mathbf{V}_0 \mathbf{b} = \mathbf{0}_L. \quad (13)$$

Similar to the minimal length case, let  $\mathbf{x}_1 = \sqrt{L} \mathbf{a}_L$ ,  $\mathbf{x}_2 = \sqrt{L} \mathbf{V}_2 \mathbf{a}_L$ , and  $\mathbf{x}_3 = \sqrt{L} \mathbf{V}_2 \mathbf{V}_1 \mathbf{a}_L + \mathbf{V}_2 \mathbf{V}_1 \mathbf{V}_0 \mathbf{b}$ . It is clear

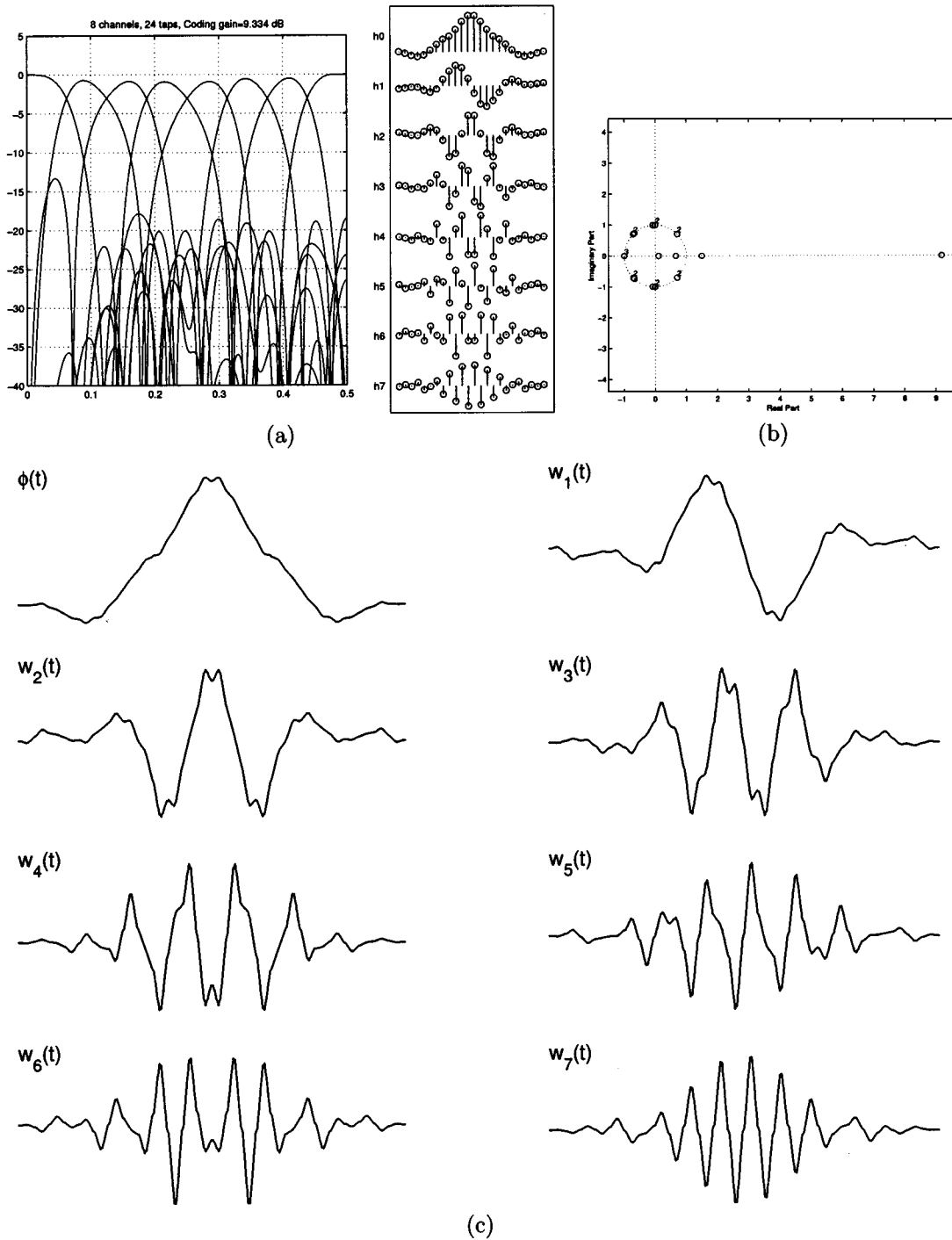


Fig. 10. Design example of two-regular minimal length PULP filterbank with  $M = 8$ , i.e., the filter length  $\ell = 24$ . (a) Frequency and impulse responses. (b) Zero locations of the lowpass filter. (c) Scaling function and wavelets.

that the vectors  $\mathbf{x}_i$  form a triangle, but unlike the previous case, the length of  $\mathbf{x}_3$  can be varied, depending on the choices of  $\mathbf{V}_0$ . In fact, it is easy to show that

$$0 \leq \|\mathbf{x}_3\| \leq \sqrt{L} + \|\mathbf{b}\|.$$

Based on the same configuration as in Fig. 7, the angles  $\lambda_1$  and  $\lambda_2$  are determined from the lengths of the three vectors. In order to form a closed triangle of the vectors  $\mathbf{x}_i$ , they must satisfy the triangle inequality, i.e.,  $||\|\mathbf{x}_1\| - \|\mathbf{x}_2\|| \leq \|\mathbf{x}_3\| \leq \|\mathbf{x}_1 + \mathbf{x}_2\|$ .

Since  $\|\mathbf{b}\| = \sqrt{(M^2 - 1)/6M} < \sqrt{L}$ , the triangle inequality becomes

$$\begin{aligned} \|\|\mathbf{x}_1\| - \|\mathbf{x}_2\|\| = 0 \leq \|\mathbf{x}_3\| \leq \|\mathbf{b}\| + \sqrt{L} &\leq 2\sqrt{L} \\ &= \|\mathbf{x}_1\| + \|\mathbf{x}_2\| \end{aligned} \quad (14)$$

and thus, (13) is always possible, regardless of the choice of  $\mathbf{V}_0$ . Similar to the previous case, we choose to impose the condition  $A_1$  into  $\mathbf{V}_1$  and  $\mathbf{V}_2$ , which means that  $\mathbf{V}_0$  is free to be chosen. The only difference between the cases of  $N = 3$  and  $N = 4$  is

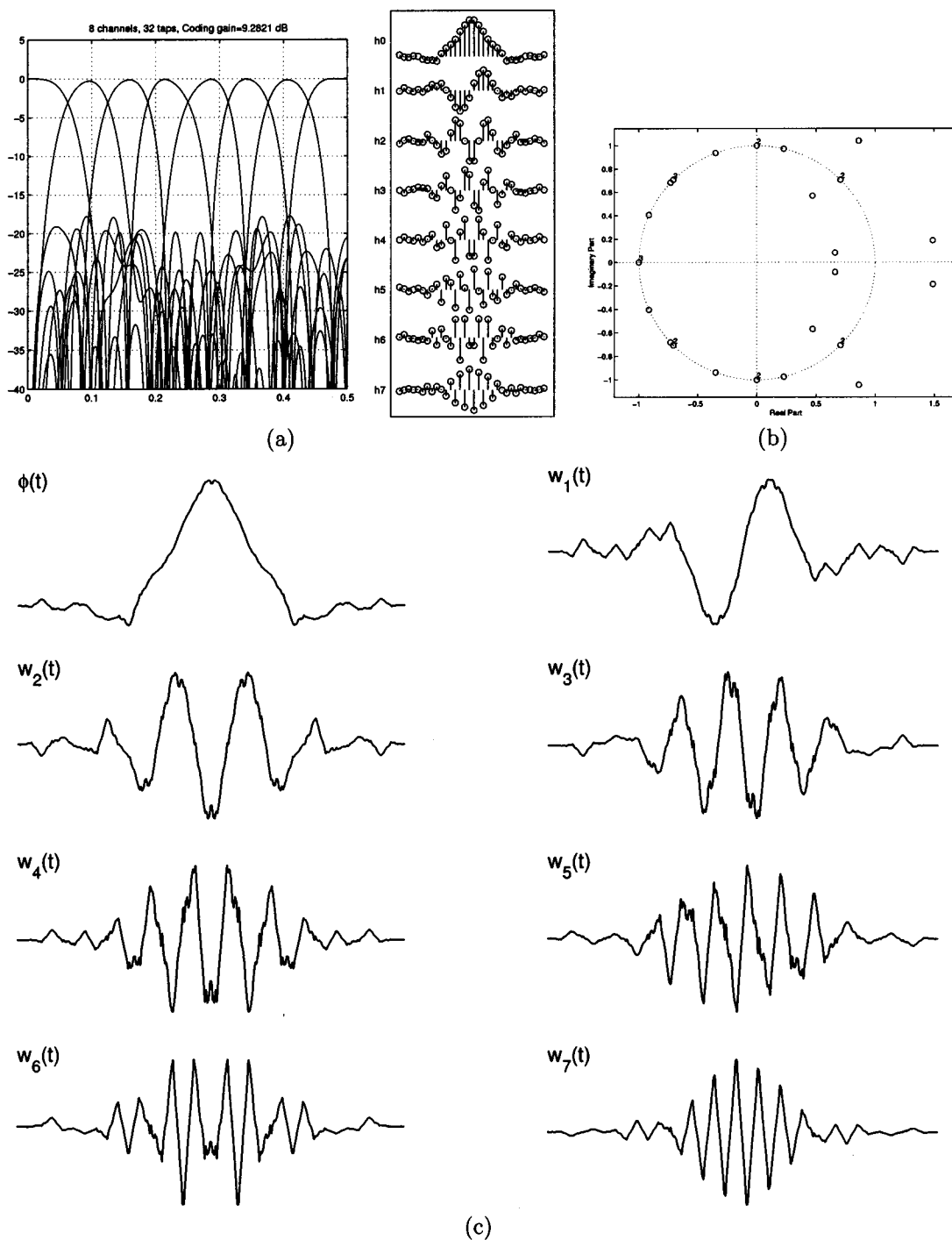


Fig. 11. Illustration of a necessary condition for the second vanishing moment and the roles of the vectors  $c_k$  and the exterior angles  $\gamma_k$ .

that, based on the notations in Fig. 7, the angles  $\lambda_1$  and  $\lambda_2$  are now dependent on  $\mathbf{x}_3$ , i.e.,

$$\lambda_1 = \cos^{-1} \left( \frac{\|\mathbf{x}_3\|}{2\sqrt{L}} \right) \quad \text{and} \quad \lambda_2 = 2\sin^{-1} \left( \frac{\|\mathbf{x}_3\|}{2\sqrt{L}} \right). \quad (15)$$

From (15), it is clear that  $\lambda = \lambda_1 + \lambda_2$  must be calculated after the vector  $\mathbf{x}_3$  is known, i.e.,  $\mathbf{V}_0$  must be already determined. Once  $\lambda$  is calculated, the  $\mathbf{V}_1$  and  $\mathbf{V}_2$  are determined in the similar manner as in the case of  $N = 3$ , whereas  $\mathbf{V}_3$  is free to be chosen since it does not depend on either condition  $A_0$  or  $A_1$ .

*Example:* In this design example, a two-regular 32-tap eight-channel PULP filterbank is designed using the proposed theory.

Its frequency response, the zeros of the lowpass filter, and the corresponding scaling and wavelet functions are, respectively, shown in Fig. 11(a)–(c).

*D. Imposing the Second Regularity: Filter Length Is Equal to  $NM$  with  $N > 4$*

From the two previous subsections, one can see that the same technique can be generalized to the case where the length of the filters is longer than  $4M(N > 4)$ . However, special treatment must be applied when the filter length is long in order to guarantee the triangle inequality. In particular, it must be satisfied by

the choices of  $\mathbf{V}_i$  at every step. Recall that the condition  $A_1$  for the general case is given by (4)

$$\sqrt{L} \mathbf{a}_L + \sqrt{L} \sum_{j=2}^{N-1} \left( \prod_{i=N-2}^{N-j} \mathbf{V}_i \right) \mathbf{a}_L + \left( \prod_{i=N-2}^0 \mathbf{V}_i \right) \mathbf{b} = \mathbf{0}_L. \quad (16)$$

From (16), it is clear that

$$\begin{aligned} & \left| \sqrt{L} \sum_{j=N-k}^{N-1} \left( \prod_{i=N-2}^{N-j} \mathbf{V}_i \right) \mathbf{a}_L + \left( \prod_{i=N-2}^0 \mathbf{V}_i \right) \mathbf{b} \right| \\ &= \sqrt{L} \left| \mathbf{a}_L + \sum_{j=2}^{N-k-1} \left( \prod_{i=N-2}^{N-j} \mathbf{V}_i \right) \mathbf{a}_L \right| \\ &\leq (N-k-1)\sqrt{L} \end{aligned} \quad (17)$$

for  $1 \leq k \leq N-3$ . This is why the first case of  $N=3$  does not need this special treatment since the left-hand side is zero. When  $N=4$ , there is only one value of  $k$ , i.e.,  $k=1$ , that needs to be checked, and since  $\|\mathbf{b}\| < \sqrt{L}$ , the inequality (17) holds, as in (14). When  $N \geq 5$ , (17) has to be taken into consideration when the matrices  $\mathbf{V}_i$  are chosen. In fact, only approximately one half of the values of  $k$  need to be checked, as stated in the following theorem.

**Theorem IV.3:** The inequalities in (17) always hold if  $k \leq \lfloor N/2 \rfloor - 1$ , where  $\lfloor x \rfloor$  is the largest integer less than or equal to  $x$ .

*Proof:* Let  $k \leq \lfloor N/2 \rfloor - 1$ . From (17), we have

$$\begin{aligned} & \left| \sqrt{L} \sum_{j=N-k}^{N-1} \left( \prod_{i=N-2}^{N-j} \mathbf{V}_i \right) \mathbf{a}_L + \left( \prod_{i=N-2}^0 \mathbf{V}_i \right) \mathbf{b} \right| \\ &\leq k\sqrt{L} + \|\mathbf{b}\| = k\sqrt{L} + \sqrt{\frac{M^2-1}{6M}} < (k+1)\sqrt{L} \\ &\leq \left\lfloor \frac{N}{2} \right\rfloor \sqrt{L} \leq \left( N - \left\lfloor \frac{N}{2} \right\rfloor \right) \sqrt{L} \leq (N-k-1)\sqrt{L}. \end{aligned}$$

Theorem IV.3 suggests that only when  $\lfloor N/2 \rfloor \leq k \leq N-3$ , (17) needs to be checked. Supposing that the matrices  $\mathbf{V}_i$  are determined in increasing order, then Theorem IV.3 implies that  $\mathbf{V}_i$  for  $i=0, \dots, \lfloor N/2 \rfloor - 2$  can be arbitrarily chosen. If  $i \geq \lfloor N/2 \rfloor - 1$ , there are some choices of  $\mathbf{V}_i$  that can violate (17), and hence, they have to be carefully chosen.

To be more concrete, for each  $k$ , let

$$\mathbf{c}_k = \sqrt{L} \sum_{j=N-k}^{N-1} \left( \prod_{i=k-1}^{N-j} \mathbf{V}_i \right) \mathbf{a}_L + \left( \prod_{i=k-1}^0 \mathbf{V}_i \right) \mathbf{b}. \quad (18)$$

Hence, (17) can be written as

$$\|\sqrt{L} \mathbf{a}_L + \mathbf{V}_k \mathbf{c}_k\| \leq (N-k-2)\sqrt{L}. \quad (19)$$

Supposing that  $\mathbf{V}_i$ , for  $i \leq k-1$  have been specified,  $\mathbf{c}_k$  can be computed. Therefore, the matrix  $\mathbf{V}_k$  has to be chosen in terms of  $\mathbf{c}_k$  so that (19) is satisfied. Let  $\gamma_k$  be the angles between  $\mathbf{V}_k \mathbf{c}_k$  and  $\mathbf{a}_L$ . Fig. 12 illustrates the roles of  $\gamma_k$ . Squaring both sides of (19) yields

$$\begin{aligned} L + \|\mathbf{c}_k\|^2 + 2\sqrt{L}\|\mathbf{c}_k\| \cos \gamma_k &\leq (N-k-2)^2 L \\ \cos \gamma_k &\leq \frac{[(N-k-1)^2 - 1]L - \|\mathbf{c}_k\|^2}{2\sqrt{L}\|\mathbf{c}_k\|}. \end{aligned}$$

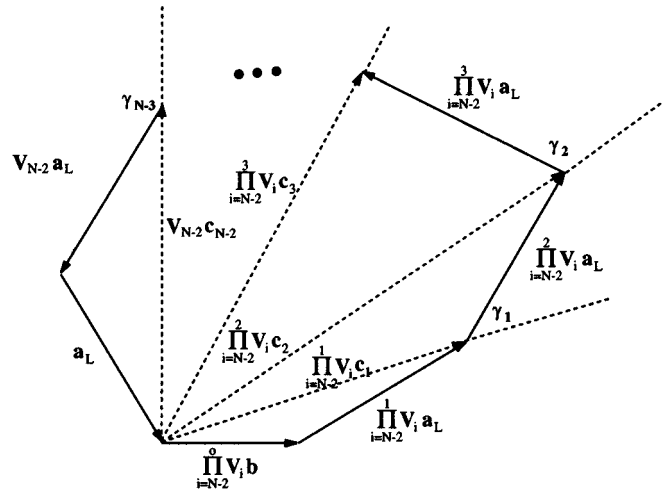


Fig. 12. Design example of two-regular minimal length PULP filterbank with  $M=8$ , i.e., the filter length  $\ell=32$ . (a) Frequency and impulse responses. (b) Zero locations of the lowpass filter. (c) Scaling function and wavelets.

(20)

Again, let us parameterize  $\mathbf{V}_k$  using the configuration presented in Fig. 8. For each  $k$ , by choosing

$$\mathbf{V}_k^0 = \mathbf{R}[\mathbf{c}_k]^T$$

the exterior angles  $\gamma_k$  can be expressed in terms of the matrices  $\mathbf{V}_k$  as follows:

$$\begin{aligned} \gamma_k &= \angle(\mathbf{a}_L, \mathbf{V}_k \mathbf{c}_k) = \angle(\mathbf{a}_L, \mathbf{V}_k^2 \mathbf{V}_k^1 \mathbf{a}_L) \\ &= \angle(\mathbf{a}_L, \mathbf{V}_k^1 \mathbf{a}_L). \end{aligned} \quad (21)$$

From Fig. 8, it is obvious that

$$\cos \theta_1 \cos \theta_2 \cdots \cos \theta_{L-1} = \cos \gamma_k. \quad (22)$$

Hence,  $\bar{\mathbf{V}}_k$  can be arbitrarily chosen, and the constraints (20) can be imposed by choosing  $\theta_j$  that satisfy (22).

## V. APPLICATION IN IMAGE COMPRESSION

In this section, the novel regular filterbanks and  $M$ -band wavelet obtained from the design examples are evaluated in an image compression application. The test images in the experiment are popular  $512 \times 512$  8-bit gray-scale images *Lena*, *Barbara*, *Goldhill*. The set partitioning in hierarchical trees (SPIHT) progressive image transmission algorithm is chosen to compare the performances of the transforms. In other words, the encoding algorithm is fixed. We only modify the decomposition stage in the encoder and the reconstruction stage in the decoder with different transformations. The five transforms chosen for the experiment are

- two-band 9/7 Daubechies symmetric wavelets [21], four degrees of regularity, six levels of iteration;
- eight-band eight-tap DCT [22], one degree of regularity, two levels of iteration;
- eight-band 16-tap LOT [23], one degree of regularity, two levels of iteration;
- eight-band 24-tap PULP regular FB labeled PULPv1, one degree of regularity, two levels of iteration;
- eight-band 24-tap PULP regular FB labeled PULPv2, two degrees of regularity, two levels of iteration.

TABLE I  
OBJECTIVE PROPERTIES OF THE PULP FILTER BANKS USED IN IMAGE  
COMPRESSION EXPERIMENTS

Transform Property	$8 \times 8$	$8 \times 16$	$8 \times 24$	$8 \times 24$
	DCT	LOT	PULPv1	PULPv2
Coding gain (dB)	8.83	9.22	9.36	9.33
Deg. of regularity	1	1	1	2
Stopband attn.(dB)	4.43	16.32	19.48	13.00

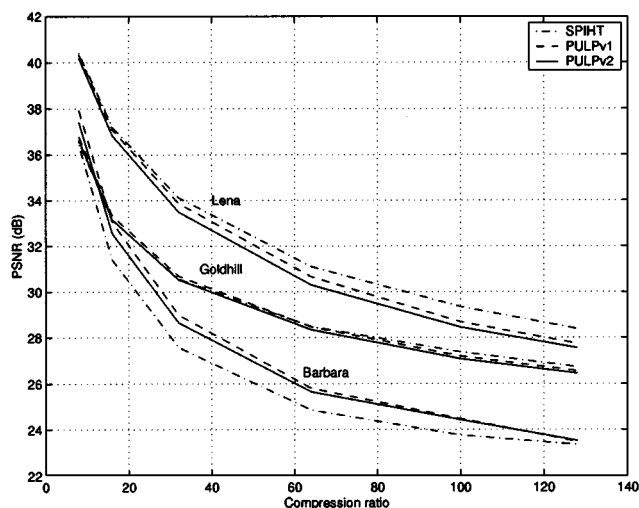


Fig. 13. PSNR of the reconstruction images using (9, 7) wavelets (dash-dot line), PULPv1 (dash line), and PULPv2 (solid line) filterbanks in the progressive image transmission coding. The transforms are tested on *Lena*, *Barbara*, and *Goldhill* images.

Table I summarizes the properties of the  $M$ -band transforms used in the comparison. For these  $M$ -band transforms, the lowpass subband coefficients are collected and fed through another stage of transformation. Since the size of the test images is limited, we can only have two levels of decomposition. To avoid modification of the encoding algorithm, the  $M$ -band wavelet coefficients are rearranged and grouped into the popular quad-tree structure (each parent node in a zero-tree has four descendants). This way, a two-level iteration of an eight-band filterbank is equivalent to a six-level dyadic wavelet iteration. For more details on the coefficient rearrangement and regrouping, see [24] and [25].

Fig. 13 shows the rate-distortion curves obtained from PULPv1 and PULPv2 filterbanks at various compression ratios ranging from 8:1 to 128:1. The full sets of PSNR values are tabulated in Table II. It is evident that the system with one vanishing moment (PULPv1) has higher objective performance comparing with that with two vanishing moments (PULPv2). However, the perceptual quality of the PULPv2 filterbank is slightly better. Fig. 14 illustrates the original and the zoom-in part of the reconstructed *Barbara* images. One can notice that in smooth regions, the PULPv1 filterbank still has a checkerboarding artifact, whereas the PULPv2 filterbank yields a smoother reconstruction. Both of these filterbanks have exactly the same level of computational complexity.

We note that length 24 is the minimum length for the two-regular eight-channel PULP filterbank. Therefore, there

TABLE II  
OBJECTIVE CODING RESULTS (PSNR in dB) USING DIFFERENT TRANSFORMS  
ON TEST IMAGES *LENA*, *BARBARA*, AND *GOLDHILL*

Lena	PSNR (dB)				
	SPIHT (9/7 WL)	$8 \times 8$ DCT	$8 \times 16$ LOT	$8 \times 24$ PULPv1	$8 \times 24$ PULPv2
1:8	40.41	39.88	40.02	40.33	40.18
1:16	37.21	36.31	36.67	37.10	36.84
1:32	34.11	32.77	33.45	33.86	33.48
1:64	31.10	29.45	30.29	30.66	30.30
1:100	29.35	27.55	28.32	28.68	28.45
1:128	28.38	26.68	27.37	27.74	27.55

Barbara	PSNR (dB)				
	SPIHT (9/7 WL)	$8 \times 8$ DCT	$8 \times 16$ LOT	$8 \times 24$ PULPv1	$8 \times 24$ PULPv2
1:8	36.41	36.29	37.40	37.92	37.41
1:16	31.40	31.07	32.66	33.04	32.55
1:32	27.58	27.21	28.72	28.99	28.65
1:64	24.86	24.48	25.58	25.81	25.65
1:100	23.76	23.33	24.23	24.48	24.43
1:128	23.35	22.53	23.22	23.48	23.52

Goldhill	PSNR (dB)				
	SPIHT (9/7 WL)	$8 \times 8$ DCT	$8 \times 16$ LOT	$8 \times 24$ PULPv1	$8 \times 24$ PULPv2
1:8	36.55	36.23	36.63	36.78	36.63
1:16	33.13	32.75	33.17	33.32	33.15
1:32	30.56	30.03	30.55	30.69	30.53
1:64	28.48	27.87	28.31	28.47	28.34
1:100	27.38	26.57	27.03	27.20	27.08
1:128	26.73	25.92	26.40	26.56	26.45

are only a few degrees of freedom left in the optimization process. The PSNR difference between the two transforms (PULPv1 and PULPv2) can be reduced by allowing longer filter length. In addition, note that the filterbanks used in the compression are optimized to reduce the stopband attenuation only, and thus, they are not yet optimal for practical image coding. There are many criteria such as transform coding gain, nonequally weighted stopband attenuation, i.e., nonconstant  $W_i(e^{j\omega})$ , mirror frequency, etc., which can improve the coding performance [24]. These will be incorporated in the design procedure of future work.

## VI. CONCLUDING REMARKS

In this paper, the theory, design, lattice structure, and coding application of PULP filterbanks with one and two degrees of

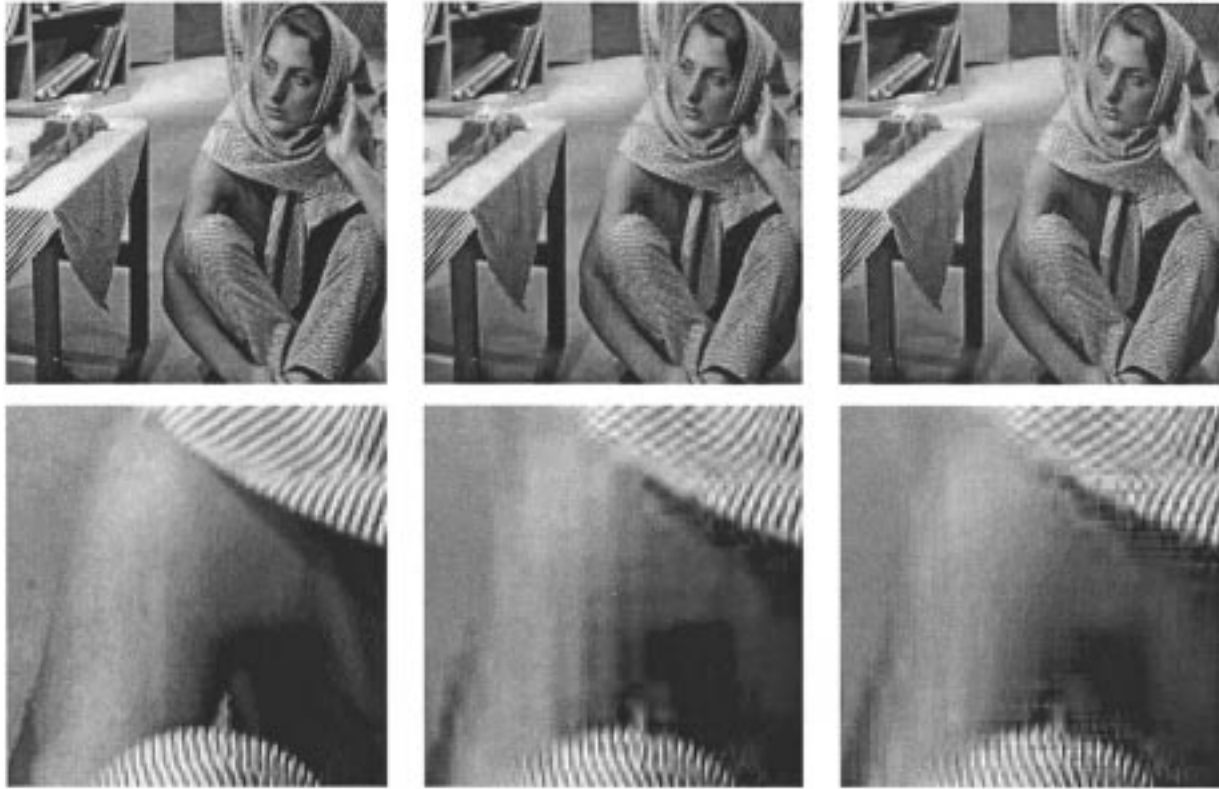


Fig. 14. Coding results at compression rate 32 : 1. The first column corresponds to the original image. The second and third columns are the images coded using an eight-band 24-tap wavelet with one and two degrees of regularity, respectively.

regularity are presented. The proposed lattice structure guarantees that the resulting filterbanks have all of the desired properties (PR, PU, LP, and one or two vanishing moments). The number of the channel  $M$  is assumed to be even, and all the filters have the same length  $NM$  for some integer  $N$ . The conditions for obtaining one and two vanishing moments from the resulting filters are derived in terms of the lattice elements. In order to design a PULP filterbank with one degree of regularity, the minimal permissible length of the filters is  $M$ , and the popular DCT satisfies this condition. It is found that  $(M/2) - 1$  rotation angles of  $\mathbf{U}_0$  can be used to enforce the first degree of regularity of the filterbank. This constraint reduces the degrees of freedom in optimizing the filterbank by  $(M/2) - 1$ .

For a PULP filterbank with two degrees of regularity, a necessary and sufficient condition of the lattice elements is derived in the general case for arbitrary filter length. Unlike the general paraunitary filterbanks that require the minimum permissible filter length to be  $2M$ , the minimum permissible length in the PULP case is proven to be  $3M$ . The design method is divided into three cases, where the filters' lengths are  $\ell = 3M$ ,  $\ell = 4M$ , and  $\ell > 4M$ . Unconstrained optimization is used in the design process. Many regular design examples are presented.

The novel filterbanks are then evaluated and compared with previously published filterbanks in the literature using a progressive image transmission coding framework. With filter length  $\ell = 24$  (which is the minimum length for two-regular eight-channel PULP filterbanks), the one with one vanishing moment yields better objective coding performance in PSNR (ranging from 0 to 1.5 dB). However, in terms of perceptual

quality, the filterbank with two vanishing moments consistently offers smoother reconstructed images.

#### APPENDIX

*Proof of Condition A<sub>1</sub>*: Substituting  $n = 1$  in (2) yields a necessary and sufficient condition for the filterbank to have two vanishing moments. Hence

$$\mathbf{v}_1 \triangleq \frac{d}{dz} \left\{ \mathbf{E}(z^M) \begin{bmatrix} 1 \\ z^{-1} \\ \vdots \\ z^{-M+1} \end{bmatrix} \right\}_{z=1} = \mathbf{v}_2 + \mathbf{v}_3 \quad (23)$$

where

$$\mathbf{v}_2 \triangleq \left. \frac{d\mathbf{E}(z^M)}{dz} \right|_{z=1} \begin{bmatrix} 1 \\ 1 \\ \vdots \\ 1 \end{bmatrix}$$

and

$$\mathbf{v}_3 \triangleq \mathbf{E}(1) \frac{d}{dz} \begin{bmatrix} 1 \\ z^{-1} \\ \vdots \\ z^{-M+1} \end{bmatrix}_{z=1}$$

$$\frac{d}{dz} [1 \ z^{-1} \ \cdots \ z^{-M+1}]_{z=1}^T = -[0 \ 1 \ \cdots \ M-1]^T \quad (24)$$

$$\mathbf{E}(1) = \mathbf{\Gamma}_{N-1} \mathbf{W} \mathbf{\Lambda}(1) \mathbf{W} \mathbf{\Gamma}_{N-2} \cdots \mathbf{\Gamma}_1 \mathbf{W} \mathbf{\Lambda}(1) \mathbf{W} \mathbf{\Gamma}_0 \mathbf{W} \mathbf{\tilde{I}} \quad (25)$$

$$= \Gamma_{N-1} \Gamma_{N-2} \cdots \Gamma_1 \Gamma_0 \tilde{\mathbf{W}} \tilde{\mathbf{I}} = \begin{bmatrix} \mathbf{U}_0 & \mathbf{0} \\ \mathbf{0} & \prod_{i=N-1}^0 \mathbf{V}_i \end{bmatrix} \tilde{\mathbf{W}} \tilde{\mathbf{I}}. \quad (26)$$

Therefore

$$\mathbf{v}_3 = \begin{bmatrix} \mathbf{v}_3^1 \\ \mathbf{v}_3^2 \end{bmatrix} \quad (27)$$

where

$$\mathbf{v}_3^1 = -\frac{M-1}{\sqrt{2}} \mathbf{U}_0 \mathbf{1}_L, \quad \mathbf{v}_3^2 = \frac{M}{\sqrt{2}} \left( \prod_{i=N-1}^0 \mathbf{V}_i \right) \mathbf{b}$$

and  $\mathbf{b} = (1/M)[M-1 \ M-3 \ \cdots \ 1]^T$ .

$$\begin{aligned} & \left. \frac{d}{dz} \mathbf{E}(z^M) \right|_{z=1} \\ &= \Gamma_{N-1} \left[ \mathbf{W} \frac{d\Lambda(z^M)}{dz} \mathbf{W} \Gamma_{N-2} \mathbf{W} \Lambda(z^M) \mathbf{W} \Gamma_{N-3} \cdots \right. \\ & \quad \Gamma_1 \mathbf{W} \Lambda(z^M) \mathbf{W} + \mathbf{W} \Lambda(z^M) \mathbf{W} \Gamma_{N-2} \mathbf{W} \\ & \quad \cdot \frac{d\Lambda(z^M)}{dz} \mathbf{W} \Gamma_{N-3} \cdots \Gamma_1 \mathbf{W} \Lambda(z^M) \mathbf{W} + \cdots \\ & \quad \left. + \mathbf{W} \Lambda(z^M) \mathbf{W} \Gamma_{N-2} \mathbf{W} \Lambda(z^M) \mathbf{W} \Gamma_{N-3} \cdots \right. \\ & \quad \left. \Gamma_1 \mathbf{W} \frac{d\Lambda(z^M)}{dz} \mathbf{W} \right] \Gamma_0 \tilde{\mathbf{W}} \tilde{\mathbf{I}} \Big|_{z=1} \\ &= \Gamma_{N-1} [\tilde{\mathbf{W}} \Gamma_{N-2} \Gamma_{N-3} \cdots \Gamma_1 + \Gamma_{N-2} \tilde{\mathbf{W}} \Gamma_{N-3} \cdots \\ & \quad \Gamma_1 + \cdots + \Gamma_{N-2} \Gamma_{N-3} \cdots \Gamma_1 \tilde{\mathbf{W}}] \Gamma_0 \tilde{\mathbf{W}} \tilde{\mathbf{I}} \end{aligned}$$

where

$$\tilde{\mathbf{W}} = \mathbf{W} \left. \frac{d\Lambda(z^M)}{dz} \right|_{z=1} \mathbf{W} = -\frac{M}{2} \begin{bmatrix} \mathbf{I}_L & -\mathbf{I}_L \\ -\mathbf{I}_L & \mathbf{I}_L \end{bmatrix}.$$

Thus

$$\begin{aligned} \mathbf{v}_2 &= \sum_{j=1}^{N-1} \begin{bmatrix} \mathbf{I} & \mathbf{0} \\ \mathbf{0} & \prod_{i=N-1}^{N-j} \mathbf{V}_i \end{bmatrix} \tilde{\mathbf{W}} \begin{bmatrix} \mathbf{U}_0 & \mathbf{0} \\ \mathbf{0} & \prod_{i=N-j-1}^0 \mathbf{V}_i \end{bmatrix} \tilde{\mathbf{W}} \tilde{\mathbf{I}} \mathbf{1}_M \\ &= -\frac{M}{\sqrt{2}} \sum_{j=1}^{N-1} \begin{bmatrix} \mathbf{U}_0 & -\prod_{i=N-j-1}^0 \mathbf{V}_i \\ -\left( \prod_{i=N-1}^{N-j} \mathbf{V}_i \right) \mathbf{U}_0 & \prod_{i=N-1}^0 \mathbf{V}_i \end{bmatrix} \begin{bmatrix} \mathbf{1}_L \\ \mathbf{0}_L \end{bmatrix} \\ &= -\frac{M}{\sqrt{2}} \sum_{j=1}^{N-1} \begin{bmatrix} \mathbf{U}_0 \mathbf{1}_L \\ -\left( \prod_{i=N-1}^{N-j} \mathbf{V}_i \right) \mathbf{U}_0 \mathbf{1}_L \end{bmatrix} \triangleq \begin{bmatrix} \mathbf{v}_2^1 \\ \mathbf{v}_2^2 \end{bmatrix} \end{aligned}$$

where we have

$$\mathbf{v}_2^1 = -\frac{M(N-1)}{\sqrt{2}} \mathbf{U}_0 \mathbf{1}_L,$$

and

$$\mathbf{v}_2^2 = \frac{M}{\sqrt{2}} \sum_{j=1}^{N-1} \left( \prod_{i=N-1}^{N-j} \mathbf{V}_i \right) \mathbf{U}_0 \mathbf{1}_L.$$

Substituting  $\mathbf{v}_2$  and  $\mathbf{v}_3$  back into (23) yields two matrix-vector equations. The first equation is obtained from equating the top half elements of all the vectors, i.e.,

$$\mathbf{v}_2^1 + \mathbf{v}_3^1 = -\frac{MN-1}{\sqrt{2}} \mathbf{U}_0 \mathbf{1}_L = \mathbf{c}_1 \mathbf{a}_L. \quad (28)$$

Notice that this equation is exactly the same as the condition  $A_0$ , which has already been imposed by enforcing the first  $L-1$  rotation angles of  $\mathbf{U}_0$ , as in Lemma 4.2.1. The second equation comes from the bottom row of (23), i.e.,

$$\begin{aligned} \mathbf{v}_2^2 + \mathbf{v}_3^2 &= \frac{M}{\sqrt{2}} \sum_{j=1}^{N-1} \left( \prod_{i=N-1}^{N-j} \mathbf{V}_i \right) \mathbf{U}_0 \mathbf{1}_L \\ &+ \frac{M}{\sqrt{2}} \left( \prod_{i=N-1}^0 \mathbf{V}_i \right) \mathbf{b} = \mathbf{0}_L. \end{aligned} \quad (29)$$

Premultiplying the above equation by  $\sqrt{2} \mathbf{V}_{N-1}^T / M$  and taking into account that  $\mathbf{U}_0 \mathbf{1}_L = \sqrt{L} \mathbf{a}_L$  results in the condition  $A_1$ , as previously described. ■

## REFERENCES

- [1] P. P. Vaidyanathan, *Multirate Systems and Filter Banks*. Englewood Cliffs, NJ: Prentice-Hall, 1993.
- [2] G. Strang and T. Nguyen, *Wavelets and Filter Banks*. Wellesley, MA: Wellesley-Cambridge, 1996.
- [3] T. D. Tran, M. Ikehara, and T. Q. Nguyen, "Linear phase paraunitary filter bank with variable-length filters and its application in image compression," *IEEE Trans. Signal Processing*, vol. 47, pp. 2730–2744, Oct. 1999.
- [4] T. D. Tran and T. Q. Nguyen, "On M-channel linear-phase FIR filter banks and application in image compression," *IEEE Trans. Signal Processing*, vol. 45, pp. 2175–2187, Sept. 1997.
- [5] L. Chen, T. Q. Nguyen, and K.-P. Chan, "Symmetric extension methods for parallel M-channel perfect-reconstruction linear-phase fir analysis/synthesis systems," *IEEE Trans. Signal Processing*, vol. 43, pp. 2505–2511, Nov. 1995.
- [6] A. K. Soman, P. P. Vaidyanathan, and T. Q. Nguyen, "Linear-phase orthogonal filter banks," *IEEE Trans. Signal Processing*, vol. 41, pp. 3480–3496, Dec. 1993.
- [7] R. L. de Queiroz, T. Q. Nguyen, and K. R. Rao, "The GenLOT: Generalized linear-phase lapped orthogonal transform," *IEEE Trans. Signal Processing*, vol. 44, pp. 497–507, Mar. 1996.
- [8] C. W. Kok, T. Nagai, M. Ikehara, and T. Q. Nguyen, "Structures and factorizations of linear phase paraunitary filter banks," in *Proc. ISPASS*, 1996.
- [9] T. Tran, R. deQueiroz, and T. Nguyen, "Linear-phase perfect reconstruction filter bank: Lattice structure, design and application in image coding," *IEEE Trans. Signal Processing*, vol. 48, pp. 133–147, Jan. 2000.
- [10] P. Steffen, P. N. Heller, R. A. Gopinath, and C. S. Burrus, "Theory of regular M-band wavelet bases," *IEEE Trans. Signal Processing*, vol. 41, pp. 3497–3510, Dec. 1993.
- [11] I. Daubechies, *Ten Lectures on Wavelets*. Philadelphia, PA: SIAM, 1992.
- [12] P. P. Vaidyanathan and P.-Q. Hoang, "Lattice structures for optimal design and robust implementation of two-channel perfect reconstruction QMF banks," *IEEE Trans. Acoust., Speech, Signal Processing*, vol. 36, pp. 81–94, Jan. 1988.
- [13] T. Q. Nguyen and P. P. Vaidyanathan, "Two-channel perfect reconstruction FIR QMF structures which yield linear phase FIR analysis and synthesis filters," *IEEE Trans. Acoust., Speech, Signal Processing*, vol. 37, pp. 676–690, May 1989.
- [14] S. Oraintara, P. Heller, T. Tran, and T. Nguyen, "Lattice structure for regular-paraunitary linear-phase filter banks," in *Proc. 2nd Int. Workshop Transforms Filter Banks*, Brandenburg an der Havel, Germany, Mar. 1999.
- [15] Y. Wisutmethangoon and T. Q. Nguyen, "A method for design of Mth-band filters," *IEEE Trans. Signal Processing*, vol. 47, pp. 1669–1678, June 1999.

- [16] P. N. Heller and H. L. Resnikoff, "Regular M-band wavelets and applications," in *ICASSP*, vol. III, 1993, pp. III-229-III-232.
- [17] J. P. Princen and A. B. Bradley, "Analysis/synthesis filter bank design based on time domain aliasing cancellation," *IEEE Trans. Acoust., Speech, Signal Processing*, vol. 34, pp. 1153-1161, 1986.
- [18] X. Q. Gao, T. Q. Nguyen, and G. Strang, "The factorization of M-channel paraunitary filter banks," *IEEE Trans. Signal Processing*, to be published.
- [19] H. Zou and A. H. Tewfik, "Discrete orthogonal M-band wavelet decompositions," in *Proc. ICASSP*, vol. 4, 1992, pp. IV-605-IV-608.
- [20] G. Strang, *Introduction to Linear Algebra*. Wellesley, MA: Wellesley-Cambridge Press, 1993.
- [21] M. Antonini, M. Barlaud, P. Mathieu, and I. Daubechies, "Image coding using wavelet transform," *IEEE Trans. Image Processing*, pp. 205-220, Apr. 1992.
- [22] K. R. Rao and P. Yip, *Discrete Cosine Transform: Algorithms, Advantages, Applications*. New York: Academic, 1990.
- [23] H. S. Malvar, *Signal Processing with Lapped Transforms*. Norwood, MA: Artech House, 1992.
- [24] T. D. Tran and T. Q. Nguyen, "A progressive transmission image coder using linear phase uniform filter banks as block transforms," *IEEE Trans. Image Processing*, vol. 48, pp. 1493-1507, Nov. 1999.
- [25] H. S. Malvar, "Fast progressive image coding without wavelets," in *Proc. Data Compression Conf.*, Snowbird, UT, Mar. 2000, pp. 243-252.



**Soontorn Oraintara** (S'97-M'00) received the B.E. degree (with first-class honors) from the King Monkut's Institute of Technology Ladkrabang, Bangkok, Thailand, in 1995 and the M.S. and Ph.D. degrees, both in electrical engineering, from the University of Wisconsin, Madison, in 1996 and Boston University, Boston, MA, in 2000, respectively.

He joined the Department of Electrical Engineering, University of Texas at Arlington, as Assistant Professor in July 2000. From May 1998 to April 2000, he was an intern and a consultant at

the Advanced Research and Development Group, Ericsson, Inc., Research Triangle park, NC. His current research interests are in the field of digital signal processing; wavelets, filterbanks and multirate systems, and their applications in data compression, signal detection and estimation, communications, image reconstruction, and regularization and noise reduction.

Dr. Oraintara received the Technology Award from Boston University for his invention on Integer DCT (with Y. J. Chen and Prof. T. Q. Nguyen) in 1999. He represented Thailand in the International Mathematical Olympiad competitions and, respectively, received the Honorable Mention Award, in Beijing, China, in 1989 and the bronze medal in Sigtuna, Sweden, in 1990.



**Trac D. Tran** (M'98) received the B.S. and M.S. degrees from the Massachusetts Institute of Technology, Cambridge, in 1994 and the Ph.D. degree from the University of Wisconsin, Madison, in 1998, all in electrical engineering.

He joined the Department of Electrical and Computer Engineering, The Johns Hopkins University, Baltimore, MD, in July 1998 as an Assistant Professor. His current research interests are in the field of digital signal processing, particularly in multirate systems, filterbanks, wavelets, transforms,

and their applications in signal representation, compression, processing, and communications.

Dr. Tran was the co-director of the 33rd Annual Conference on Information Sciences and Systems (CISS'99), Baltimore, MD, in March 1999. He received the NSF CAREER award in 2001.



**Peter Niels Heller** (M'91) received the B.S. degree in mathematics with highest honors from the University of North Carolina, Chapel Hill, in 1981 and the M.A. and Ph.D. degrees in mathematics from Princeton University, Princeton, NJ, in 1983 and 1986, respectively.

He is currently Chief Scientist at Aware, Inc., Bedford, MA. From 1985 through 1986, he was a CLE Moore Instructor of Mathematics at the Massachusetts Institute of Technology (MIT), Cambridge, and returned to MIT as a Visiting Lecturer in Mathematics in 1989. During 1990, he developed geometric modeling software at Parametric Technology Corp., Waltham, MA; in December 1990, he joined Aware Inc. In 1994, he co-presented the Nordic postgraduate course on wavelets, filterbanks, and applications at Helsinki University of Technology, Helsinki, Finland. His research interests include wavelets and multirate systems and their application to telecommunications and data compression. At Aware, he directs the development of broadband modem chips, particularly for wireline applications such as ADSL.

Dr. Heller held NSF and Sloan Foundation Fellowships while a graduate student at Princeton.

**Truong Q. Nguyen** (SM'95) received the B.S., M.S., and Ph.D. degrees in electrical engineering from the California Institute of Technology, Pasadena, in 1985, 1986, and 1989, respectively.

He was with Lincoln Laboratory, Massachusetts Institute of Technology (MIT), Lexington, from June 1989 to July 1994, as a member of technical staff. From 1993 to 1994, he was a visiting lecturer at MIT and an adjunct professor at Northeastern University, Boston, MA. Since August 1994 to July 1998, he was with the Electrical and Computer Engineering Department, University of Wisconsin, Madison. He was with Boston University, Boston, MA, from 1996 to 2001. He is now a Full Professor at University of California at San Diego, La Jolla. His research interests are in the theory of wavelets and filterbanks and applications in image and video compression, telecommunications, bioinformatics, medical imaging and enhancement, and analog/digital conversion. He is the coauthor (with Prof. G. Strang) of a popular textbook *Wavelets and Filter Banks* (Welleley, MA: Wellesley-Cambridge, 1997) and the author of several MATLAB-based toolboxes on image compression, electrocardiogram compression, and filterbank design. He also holds a patent on an efficient design method for wavelets and filterbanks and several patents on wavelet applications, including compression and signal analysis.

Prof. Nguyen received the IEEE TRANSACTIONS ON SIGNAL PROCESSING Paper Award (in the Image and Multidimensional Processing area) for the paper he co-wrote with Prof. P. P. Vaidyanathan on linear-phase perfect-reconstruction filter banks in 1992. He received the NSF Career Award in 1995 and is currently the Series Editor (Digital Signal Processing) for Academic Press. He served as Associate Editor for the IEEE TRANSACTIONS ON SIGNAL PROCESSING from 1994 to 1996 and for the IEEE TRANSACTIONS ON CIRCUITS AND SYSTEMS from 1996 to 1997. He received the Technology Award from Boston University for his invention on Integer DCT (with Y. J. Chen and S. Oraintara). He co-organizes (with Prof. G. Strang at MIT) several Workshops on Wavelets and served on the DSP Technical Committee for the IEEE CAS society.